Constructing various paraxial beams out of regular and modified Bessel-Gaussian modes

Tomasz Radożycki *

Faculty of Mathematics and Natural Sciences, College of Sciences, Institute of Physical Sciences, Cardinal Stefan Wyszyński University, Wóycickiego 1/3, 01-938 Warsaw, Poland

(Received 7 November 2022; accepted 1 February 2023; published 13 February 2023)

Various superpositions of Bessel-Gaussian beams and modified Bessel-Gaussian beams are considered. Two selected parameters characterizing these beams, with respect to which the superpositions are constructed, are the topological index n associated with the orbital angular momentum carried by the beam and χ related to the dilation of the beam. It is shown that, from these modes, by choosing appropriate weighting factors, it is possible to create a number of well- and less-known solutions of the paraxial equation: a Gaussian (shifted and nonshifted) beam, a γ beam, Kummer-Gaussian beam, a special hyperbolic Bessel-Gaussian beam, a certain special Laguerre-Gaussian beam, and generalized paraxial beams in hyperbolic and regular versions.

DOI: 10.1103/PhysRevA.107.023510

I. INTRODUCTION

Since the first solution of the Helmholtz paraxial equation in the form of the Gaussian beam [1–11] was reported, a great variety of other beams with more complicated structures have been analytically derived and then experimentally generated. Although the Gaussian beam, i.e., the so-called fundamental mode, in many situations accurately describes the laser field that exhibits cylindrical symmetry, many practical applications require somewhat more complex patterns. We mention here other cylindrical beams such as regular Bessel-Gaussian (BG) beams [11–15] or modified Bessel-Gaussian (MBG) beams [16] and Laguerre-Gaussian (LG) beams [3,11,15,17–21] of various orders which exhibit ringlike structure and Kummer-Gaussian (KG), i.e., hypergeometric Gaussian, beams [22,23] or noncylindrical beams, for instance, Hermite-Gaussian ones [1,3] or more general paraxial beams [24]. Due to their numerous applications ranging from pure physics to optical communication technologies and image processing to biology and medicine [25–34], structured light has earned extensive literature, with the works cited above being only a sample.

The plethora of miscellaneous beams requires a kind of ordering and establishing some relationships between them. Several efforts to unify the derivation and the description of the paraxial beams have been made in the past [35–38]. In our previous work [39] we proceeded along these lines, attempting to exploit the Hankel transformation [40,41] for this purpose. The present work is in a sense devoted to a similar issue, albeit from a different point of view.

From a mathematical perspective all of the mentioned modes constitute certain exact solutions of the Helmholtz paraxial equation, which by itself has already been approximated but perfectly describes laser beams near the optical axis [3,42]:

$$\triangle_{\perp}\psi(\boldsymbol{r}, z) + 2ik\partial_z\psi(\boldsymbol{r}, z) = 0. \tag{1}$$

The scalar function $\psi(\boldsymbol{r}, z)$ proportional to the field strength we focus on in this paper is called the envelope. The Laplace operator $\triangle_{\perp}$ appearing in (1) is a two-dimensional one acting in the transverse plane only (i.e., $\boldsymbol{r} = [x, y]$) and the symbol ∂_z stands for the partial derivative $\frac{\partial}{\partial z}$ (and similarly for other variables).

The two solutions to this equation that will serve as basic ones in this work are MBG and BG modes. They play an important role due to their almost nondiffractive character and numerous applications, for instance, for harmonic generation in nonlinear optics. The expressions describing these modes are well known and are given by the formulas (2) and (37).

The BG and MBG beams have one advantage (from the point of view of a theoretical description, but also practical applications) over Gaussian beams: It is the occurrence, apart from the orbital angular momentum index n, of an additional parameter χ, which can provide an extra basis for the formation of certain new superpositions. Its appearance in the case of the BG beam is a consequence of its design out of Gaussian beams, as discussed below, in which the latter are characterized by the double opening angle, that associated with the diffraction of constitutive Gaussian beams and also their angle of inclination with respect to the z axis. In the case of the MBG beams, the role of the latter angle is played by the radius of the cylinder on which the wave vectors are distributed.

When dealing with BG and MBG beams in the rest of the paper, we ignore normalization factors. While this does not affect the conclusions drawn from the calculations, it greatly simplifies the emerging expressions. In general, the normalization factors N are rather complicated functions of the parameters χ and n (among others). Including them in superpositions would merely lead to redefinitions and unnecessary complications of the weighting factors ($w \mapsto w/N$), without affecting any meaningful conclusions. The same remark also

*t.radozycki@uksw.edu.pl

applies to other beams occurring in this work. Consequently, any comments on the behavior of expressions describing a given beam for large values of χ or n therefore refer to *unnormalized* expressions explicitly stated in the work. The experimental realization of the interference of waves requires a separate adjustment of their relative intensities anyway.

The next two sections present a series of superpositions leading to other beams known from the literature. We start in Sec. II by providing superpositions of MBG beams, owing to the fact that they exhibit better convergence properties as $\chi \to \infty$ than BG beams do, due to the presence of the factor $\exp[-\chi^2/\alpha(z)]$. For the latter beams, dealt with in Sec. III, the sign of this exponent is inverted, which necessitates the inclusion of an additional Gaussian damping function in the weighing factors and consequently precludes superpositions in which these factors are purely power law in nature. For the two most transparent cases, the effect of superposition is visualized in the figures.

II. SUPERPOSITIONS OF MODIFIED BESSEL-GAUSSIAN BEAMS

The modified Bessel-Gaussian beam of nth order has the form

$$\Psi^{(n)}_{\mathrm{MBG}}(r,\varphi,z) = \frac{2}{\alpha(z)} e^{in\varphi} e^{-(\chi^2+r^2)/\alpha(z)} I_n\left(\frac{2\chi r}{\alpha(z)}\right), \quad (2)$$

where, as mentioned in the Introduction, the normalization factor has been omitted. Here

$$\alpha(z) = w_0^2 + 2i\frac{z}{k} = w_0^2\left(1 + i\frac{z}{z_R}\right) \quad (3)$$

is the complex beam parameter, r stands for $\sqrt{x^2+y^2}$, w_0 denotes the beam waist, i.e., the distance from the propagation axis at which the irradiance weakens e^2 times, which is specified by the Gaussian factor, and $z_R = kw_0^2/2$ is the Rayleigh length, i.e., the distance at which the perpendicular area πw_0^2 related to this Gaussian factor duplicates. These quantities recur below in all beams containing a Gaussian factor, although their meaning may vary slightly from case to case.

The MBG beam can be constructed as equal-weight superpositions of Gaussian beams (4) but with foci located on a circle of radius χ [16]. The parameter χ is then arbitrary and remains at our disposal (formally from zero to infinity, but in a realistic experimental situation some truncation must occur) in the sense that expression (2) constitutes the solution of the paraxial equation regardless of its value. This property allows for constructing further superpositions of modes with differing values of χ and with weighting factors that can be χ dependent. The other kind of superposition is obtained by interfering modes with equal χ and varying values of the topological index n.

A. Gaussian beam

The nth-order Gaussian beam has the well-known form

$$\Psi^{(n)}_{G}(r,\varphi,z) = \frac{1}{\alpha(z)^{n+1}} r^n e^{in\varphi} e^{-r^2/\alpha(z)}, \quad (4)$$

where $\alpha(z)$ is defined in (3). In this section it is first demonstrated that the sum of the cofocal MBG modes (2) with appropriate χ-dependent weights restores the Gaussian beam, in general, with focus shifted along the z axis and/or of modified waist value.

Let us consider the superposition obtained by integrating over the parameter χ with relative amplitudes chosen in the form

$$\Psi_s(r,\varphi,z) \overset{\mathrm{def}}{=} \int_0^\infty d\chi \left(\frac{\chi}{\kappa}\right)^{n+1} e^{-\chi^2/\kappa} \Psi^{(n)}_{\mathrm{MBG}}(r,\varphi,z). \quad (5)$$

The quantity κ is a certain constant (satisfying the condition $w_0^2 + \mathrm{Re}\,\kappa > 0$), the interpretation of which will be given later, and the subscript s here and below stands for superimposed.

Apparently this expression seems to be singular as $\kappa \to 0$, but the close examination shows that this limit is well defined, which is owed to the behavior of the Bessel function I_n close to the origin. This is confirmed by the explicit calculation below.

Substituting the expression (2) into (5) and using the well-known integral convergent for $\mathrm{Re}a > 0$, which takes the simple form for natural n [43],

$$\int_0^\infty dx\, x^{n+1} e^{-ax^2} I_n(bx) = \frac{b^n}{(2a)^{n+1}} e^{b^2/4a}, \quad (6)$$

where it can be set

$$a = \frac{1}{\kappa} + \frac{1}{\alpha(z)}, \quad b = \frac{2r}{\alpha(z)}, \quad (7)$$

we obtain

$$\Psi_s(r,\varphi,z) = \frac{1}{[\alpha(z)+\kappa]^{n+1}} r^n e^{in\varphi} e^{-r^2/[\alpha(z)+\kappa]}. \quad (8)$$

This expression represents the standard form of the nth-order Gaussian beam (4) with the complex parameter $\alpha(z)$ shifted by κ:

$$\alpha(z) \longmapsto \alpha(z) + \kappa. \quad (9)$$

Referring to the formula (3), it is clear that the real part of κ merely modifies the beam waist and the imaginary part is responsible for the shift of the beam along the z axis,

$$w_0^2 \longmapsto w_0^2 + \mathrm{Re}\kappa, \quad z \longmapsto z + \tfrac{1}{2}k\,\mathrm{Im}\kappa, \quad (10)$$

i.e., the new focus is located in the plane $z = -\frac{1}{2}k\,\mathrm{Im}\kappa$. These results are understood on the grounds of geometrical and physical considerations. Due to the presence of the factor $\exp[-\chi^2(\frac{1}{\kappa} + \frac{1}{\alpha(z)})]$ under the integral, the values of the expression in parentheses that are significantly distinct from zero substantially contribute to the integration only in the region of small χ, either owing to the Gaussian nature of the integrand function (real part) or due to its fast oscillations (imaginary part) which entail destructive interference. Tiny values of χ, according to the geometric interpretation provided earlier, correspond to beams focused close to the z axis. The maximum of the irradiance should therefore, at least for $n = 0$, occur at a spot located on the z axis for which $z = -\frac{1}{2}k\,\mathrm{Im}\kappa$ [if $n \neq 0$ the factor r^n in (4) modifies the behavior close to the z axis so that the ring of maximal intensity around this point is created], characterized by the new waist size of $\sqrt{w_0^2 + \mathrm{Re}\kappa}$.

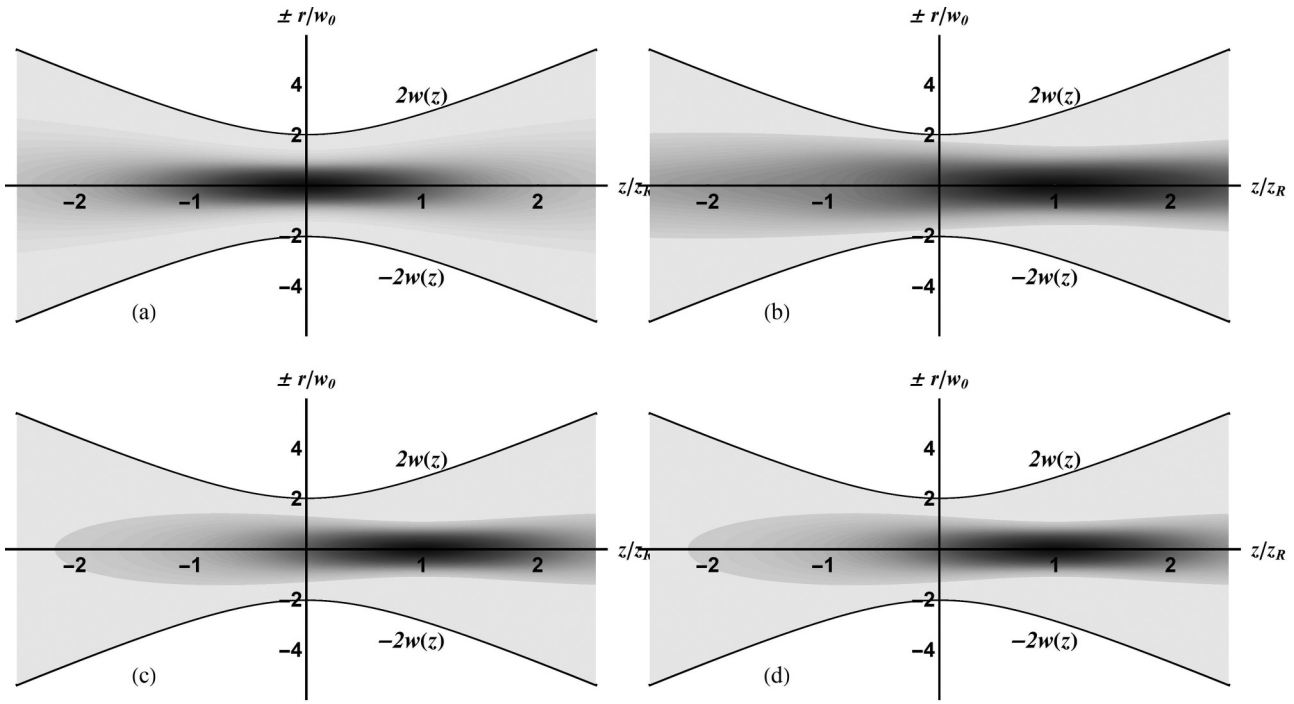

FIG. 1. Intensity of superimposed MBG beams, according to the formula (5) for $n = 0$ and $\kappa = -2iz_R/k$ in the cut plane containing the propagation axis. Subsequent plots are performed for increasing number of superimposed modes: (a) one mode with $\chi = 0.01z_R$, (b) ten modes with $\chi = 0.01z_R, 0.02z_R, \ldots, 0.1z_R$, (c) 100 modes with $\chi = 0.01z_R, 0.02z_R, \ldots, 1z_R$, and (d) 2000 modes with $\chi = 0.01z_R, 0.02z_R, \ldots, 20z_R$. The images are drawn in negative form for better visibility: Black corresponds to high and white to low intensity. Auxiliary lines $\pm 2w(z)$ are drawn as well.

These effects are demonstrated in Figs. 1 and 2 for $n = 0$ and 2, respectively. The superpositions of 1, 10, 100, and 2000 modes with weighting factors taken from the formula (5) and uniformly distributed with respect to χ (to avoid modifying these weighing factors) are created. The visible effect is the appearance of the irradiance maximum close to $z = z_R$. This

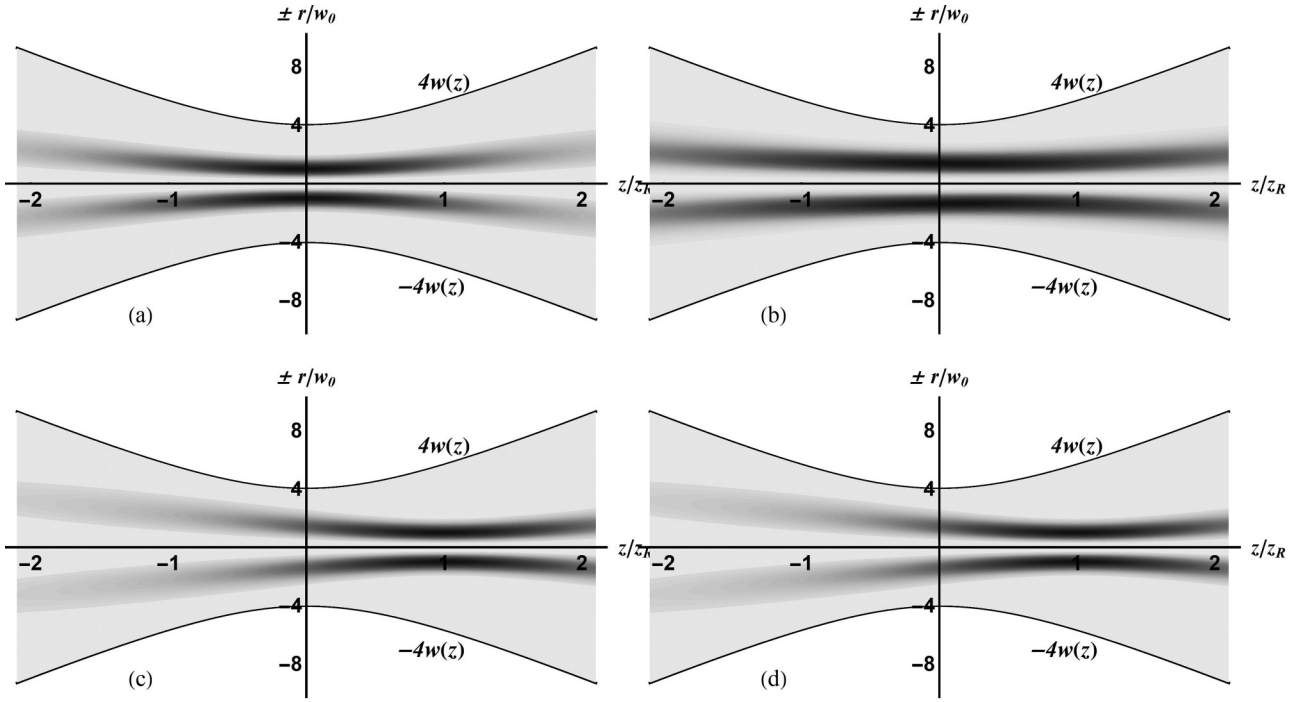

FIG. 2. Same as Fig. 1 but for $n = 2$ and auxiliary lines corresponding to $\pm 4w(z)$.

remains in line with our formulas, since the parameter κ is chosen in figures to be equal to $-2iz_R/k$, which, according to (10), leads to the shift of the Gaussian-beam focus along the propagation axis to $z = z_R$.

Let us now consider the superposition of cofocal MBG modes with fixed χ but bearing different topological indices n and weighted by factors in the form of e^{nv}, with v a parameter. Thus, let us define

$$\Psi_s(r, \varphi, z) \stackrel{\text{def}}{=} \sum_{n=-\infty}^{\infty} e^{nv} \Psi^{(n)}_{\text{MBG}}(r, \varphi, z). \tag{11}$$

Using (2), this sum can be expanded as

$$\Psi_s(r, \varphi, z) = \frac{2}{\alpha(z)} e^{-(\chi^2+r^2)/\alpha(z)} \sum_{n=-\infty}^{\infty} e^{n(v+i\varphi)} I_n\left(\frac{2\chi r}{\alpha(z)}\right). \tag{12}$$

The well-known expression for the generating function for modified Bessel functions [44]

$$e^{[z/2](t+1/t)} = \sum_{n=-\infty}^{\infty} I_n(z) t^n \tag{13}$$

allows us to rewrite (12) in the compact form

$$\begin{aligned}\Psi_s(r, \varphi, z) &= \frac{2}{\alpha(z)} e^{-(\chi^2+r^2)/\alpha(z)} \\ &\quad \times e^{[2\chi r/\alpha(z)](\cos\varphi \cosh v + i \sin\varphi \sinh v)} \\ &= \frac{2}{\alpha(z)} e^{-[1/\alpha(z)][(x-\chi\cosh v)^2+(y-i\chi\sinh v)^2]} \\ &= \Psi^{(0)}_{G\,\text{sh}}(r, \varphi, z).\end{aligned} \tag{14}$$

The obtained expression is known to represent the so-called shifted Gaussian beam [45] (this is what sh stands for) of zeroth order. For real values of v the shift in the x direction is real and that in the y direction imaginary. In this derivation, however, nothing prevents us from using complex values of v. A purely imaginary value, i.e., $v = i\beta$, for a certain real angle β shifts the focus radially by the vector $\chi[\cos\beta, \sin\beta]$. Complex shifts in general lead to slanted beams in some aspects similar to that in Fig. 2 of [46].

Thus (11) and (14) entail that the shifted Gaussian zeroth-order beam can be expressed as the superposition of cofocused MBG modes with weights given in terms of the exponential function e^{nv}. In order to clarify the underlying mechanism, suppose for definiteness that v is real and positive and for simplicity consider the plane $z = 0$. According to the formula (14), the peak of irradiance is shifted from the origin of the system along the x axis toward positive values. This effect can be understood when considering the model function

$$f_n(r, \varphi) = e^{nv} e^{in\varphi} e^{-ar^2} I_n(br), \tag{15}$$

where a and b are certain positive constants. It is obvious that the expression $e^{-ar^2} I_n(br)$ exhibits a maximum for some positive value of r. The requirement of the derivative to vanish at this point yields the equation

$$\frac{I_n'(br)}{I_n(br)} = \frac{2a}{b} r. \tag{16}$$

With increasing n the left-hand side increases as well, which can be easily seen if one uses two well-known identities [47]

$$I_n'(z) = \tfrac{1}{2}[I_{n+1}(z) + I_{n-1}(z)], \tag{17a}$$

$$2nI_n(z) = z[I_{n-1}(z) - I_{n+1}(z)]. \tag{17b}$$

They allow us to rewrite (16) in the form

$$\frac{I_{n+1}(br)}{I_n(br)} + \frac{n}{br} = \frac{2a}{b} r \tag{18}$$

and due to the positivity of the modified Bessel functions of the first kind (for positive arguments) entails the inequality

$$r^2 > \frac{n}{2a}. \tag{19}$$

At least starting from a certain value of n, the location of the maximum increases with n.

Now comparing the left ($x < 0$) and right ($x > 0$) half planes, one observes the appearance of destructive interference for the former [in particular, the factor $e^{in\varphi}$ in (15) equals $(-1)^n$ on the negative-x semiaxis] and constructive interference for the latter. The irradiance maximum is then shifted to the right. For larger values of n the maxima of the subsequent terms in the sum (11) move further and further to the right, as we have established above, and participate with substantially greater weighting factors e^{nv}. Consequently, larger values of the parameter v lead to an increasingly distant location of the irradiance peak, which is expressed in the formula (14) by the presence of the function $\cosh v$.

B. The γ beam

The weighting factor chosen under the integral (5) is not unique and remains at our disposal provided the convergence of this integral with respect to χ is ensured. Let us then set it in the form of $1/\chi^{n-1}$ and again superimpose the cofocal MBG beams, additionally assuming that $n \geqslant 2$, i.e,

$$\Psi_s(r, \varphi, z) \stackrel{\text{def}}{=} \int_0^{\infty} d\chi \frac{1}{\chi^{n-1}} \Psi^{(n)}_{\text{MBG}}(r, \varphi, z). \tag{20}$$

After plugging in the expression for $\Psi^{(n)}_{\text{MBG}}$, the above integral can be executed with the use of the known formula [43]

$$\int_0^{\infty} dx \frac{1}{x^{n-1}} e^{-ax^2} I_n(bx) = \frac{(2a)^{n-1}}{(n-1)! b^n} e^{b^2/4a} \gamma\left(n, \frac{b^2}{4a}\right), \tag{21}$$

where $\text{Re}a > 0$ and $\gamma(n, z)$ stands for the incomplete γ function [44]. In the following $\text{Re}a > 0$ is assumed. If the normalizability in the transverse plane is to be maintained, the condition $n \geqslant 2$ has to be imposed due to the asymptotic behavior of the γ function

$$\gamma(n, w) \sim \gamma_{\text{as}}(n, w) := \Gamma(n) - w^{n-1} e^{-w}, \tag{22}$$

where the index as indicates asymptotic.

Plugging the expression for $\Psi^{(n)}_{\text{MBG}}(r, \varphi, z)$ into (20) and using (21), we obtain the result in the form

$$\Psi_s(r, \varphi, z) = \frac{1}{(n-1)! r^n} e^{in\varphi} \gamma\left(n, \frac{r^2}{\alpha(z)}\right). \tag{23}$$

Apart from the inessential multiplicative constant, this expression represents the so-called γ beam [48].

It should be mentioned that the γ beam does not exhibit the Gaussian behavior but rather the power-law decay $1/r^n$ (for very large r). This is a consequence of the circumstance that in this case the superposed modes are those whose irradiance maximum is distributed over a ring with the radius growing with χ. The exemplary integral for $z = 0$ may be rewritten as

$$\int_0^\infty d\chi \frac{1}{\chi^{n-1}} I_n\left(\frac{2\chi r}{w_0^2}\right) e^{-(\chi^2+r^2)/w_0^2} = \int_0^\infty d\chi \frac{1}{\chi^{n-1}} \left[e^{-2\chi r/w_0^2} I_n\left(\frac{2\chi r}{w_0^2}\right)\right] e^{-(r-\chi)^2/w_0^2}. \quad (24)$$

The presence of the Gaussian factor ensures that for a given r the significant contribution to the integral only comes from modes where $\chi \approx r$ with a spread of several w_0. For large r, which we are concerned with, this implies that $2\chi r \gg w_0^2$ and the expression in square brackets can be approximated by $w_0/2\pi r$ [47]. Consequently, the value of the integral is proportional to $(1/r^{n-1})(1/r) = 1/r^n$. This clarifies the interference mechanism between various MBG beams, i.e., exhibiting Gaussian fall-off, which finally leads to the power-law decline.

C. Kummer-Gaussian beam

A somewhat more general integral [43]

$$\int_0^\infty dx \frac{1}{x^l} e^{-ax^2} I_n(bx) = \frac{\Gamma(\frac{n-l+1}{2}) b^n}{n! 2^{n+1} a^{(n-l+1)/2}} {}_1F_1\left(\frac{n-l+1}{2}, n+1, \frac{b^2}{4a}\right), \quad (25)$$

where $n - l > -1$, may be applied to derive the superposition of MBG modes producing the so-called Kummer-Gaussian beam introduced in [39]:

$$\Psi_s(r,\varphi,z) \overset{\text{def}}{=} \int_0^\infty d\chi \frac{1}{\chi^l} \Psi^{(n)}_{\text{MBG}}(r,\varphi,z) = \frac{\Gamma(\frac{n-l+1}{2})}{n!} \frac{1}{\alpha(z)^{(n+l+1)/2}} r^n e^{in\varphi} \times {}_1F_1\left(\frac{n-l+1}{2}, n+1, \frac{r^2}{\alpha(z)}\right) e^{-r^2/\alpha(z)}. \quad (26)$$

The interference mechanism is similar to that leading to the γ beam.

D. Special hyperbolic Bessel-Gaussian beam

Yet another integral that can be used has the form [43]

$$\int_0^\infty dx\, e^{-ax^2} I_n(bx) = \sqrt{\frac{\pi}{4a}} I_{n/2}\left(\frac{b^2}{8a}\right) e^{b^2/8a}. \quad (27)$$

Let us exploit this formula by constructing the superposition of $\Psi^{(n)}_{\text{MBG}}$'s with additional Gaussian weighting factor $e^{-\chi^2/\kappa}$, i.e., defining

$$\Psi_s(r,\varphi,z) \overset{\text{def}}{=} \int_0^\infty d\chi\, e^{-\chi^2/\kappa} \Psi^{(n)}_{\text{MBG}}(r,\varphi,z), \quad (28)$$

where κ satisfies the same convergence condition as in (5). Applying (27), we get

$$\Psi_s(r,\varphi,z) = \sqrt{\frac{\pi\kappa}{\alpha(z)(\alpha(z)+\kappa)}} e^{in\varphi} \times \exp\left(-\frac{r^2}{2\alpha(z)} \frac{2\alpha(z)+\kappa}{\alpha(z)+\kappa}\right) \times I_{n/2}\left(\frac{\kappa r^2}{2\alpha(z)(\alpha(z)+\kappa)}\right). \quad (29)$$

The halved index of the Bessel function is characteristic of a beam provisionally termed special hyperbolic Bessel-Gaussian beam in [49]. In order to transform this expression into the preferred form, i.e., the formula (14) of [49] up to a normalization constant, it is sufficient to redefine the constants as (for real κ)

$$w_0^2 \longmapsto w_0^2 - \frac{\kappa}{2}, \quad \kappa \longmapsto 2\chi. \quad (30)$$

The designation of the parameter χ occurring above is copied from the cited paper and has no relation to the integration variable of the formula (28). In the Appendix the expression (29) is derived again by directly solving the paraxial equation.

E. Generalized (hyperbolic) paraxial beam

The following summation formula for the products of modified Bessel functions holds [50]:

$$\sum_{n=-\infty}^{\infty} e^{in\varphi} I_n(u) I_{m+n}(w) = \left(\frac{w+ue^{-i\varphi}}{w+ue^{i\varphi}}\right)^{m/2} \times I_m(\sqrt{w^2+u^2+2uw\cos\varphi}). \quad (31)$$

It will be used below to derive the expansion of the generalized paraxial beam (which does not exhibit cylindrical character) onto cylindrical modified BG beams. Let us first substitute

$$u = \mu, \quad w = \frac{2\chi r}{\alpha(z)}, \quad (32)$$

where μ and χ are certain, possibly also complex, constants, and create the superposition of MBG modes over the orbital angular momentum index n with weights that in turn are modified Bessel functions of μ.

Using (31) we find the needed sum

$$\sum_{n=-\infty}^{\infty} e^{in\varphi} I_n(\mu) I_{m+n}\left(\frac{2\chi r}{\alpha(z)}\right) = e^{-im\varphi} \left(\frac{\xi(x,y,z)}{\eta(x,y,z)}\right)^m \times I_m(\xi(x,y,z)\eta(x,y,z)), \quad (33)$$

where

$$\xi(x,y,z) = \left(\mu + \frac{2\chi}{\alpha(z)}(x+iy)\right)^{1/2}, \quad (34a)$$

$$\eta(x,y,z) = \left(\mu + \frac{2\chi}{\alpha(z)}(x-iy)\right)^{1/2}. \quad (34b)$$

Now, multiplying both sides of (33) by the factor

$$\frac{1}{\alpha(z)} e^{-(r^2+\chi^2)/\alpha(z)+im\varphi} \quad (35)$$

and shifting the dummy summation variable n by $-m$, we arrive at the simple superposition formula mentioned above,

$$\Psi_s^{(m)}(x,y,z) = \frac{1}{\alpha(z)} e^{-(r^2+\chi^2)/\alpha(z)} \left(\frac{\xi(x,y,z)}{\eta(x,y,z)}\right)^m \times I_m(\xi(x,y,z)\eta(x,y,z)) = (-1)^m \sum_{n=-\infty}^{\infty} I_{n-m}(\mu)\Psi_{\mathrm{MBG}}^{(n)}(r,\varphi,z). \quad (36)$$

This expression represents a beam found in [24] by explicit solution of the paraxial equation and independently constructed from shifted Gaussian beams. Now its expansion onto MBG modes is found. It can be referred to as a generalized or few-parameter hyperbolic paraxial beam since by a suitable choice of the parameters μ and χ some of the standard beams can be obtained. In particular, the former is responsible for the noncylindrical shape of the intersection by some perpendicular plane. It becomes more and more axisymmetric when μ tends to zero (but paradoxically also when $\mu \to \infty$, since then in regions where the symmetry would be broken the wave is damped by the Gaussian factor).

III. SUPERPOSITIONS OF BESSEL-GAUSSIAN BEAMS

Regular Bessel-Gaussian beams exhibit different character, which manifests through the existence of concentric rings of higher irradiance in the planes $z = \text{const}$. Beams of nth order are described with the formula [13]

$$\Psi_{\mathrm{BG}}^{(n)}(r,\varphi,z) = \frac{2}{\alpha(z)} e^{in\varphi} e^{(\chi^2-r^2)/\alpha(z)} J_n\left(\frac{2\chi r}{\alpha(z)}\right). \quad (37)$$

As before, two parameters can be used to build superpositions: the continuous parameter χ and the discrete one n. Superpositions of this kind of mode with respect to the parameter χ are however somewhat more problematic than those for modified BG beams due to the positive sign in the exponent $e^{\chi^2/\alpha(z)}$ [recall that the real part of $\alpha(z)$ is always positive]. This unwanted sign precludes all the weighting factors that exhibit the power-law behavior, i.e., without Gaussians, that could potentially save the convergence of the infinite integral. Therefore, one has to inevitably introduce into the amplitudes the additional Gaussian factor in order to overcome the divergence at infinity. For this reason, it is not feasible to get γ or Kummer-Gaussian beams from superpositions over the parameter χ, where weighting factors would need to be purely power ones.

The BG beam (37) can be constructed by superimposing slanted Gaussian beams [16]. In this case the parameter χ, unlike in Sec. II, is now associated with the semiaperture angle of the constituent Gaussian beams and the Rayleigh length. It differs by the factor z_R/k [51,52] from the parameter β of [13,16]. Hence, there is no formal restriction on extending the superposition over χ to the entire positive semiaxis.

A. Gaussian beam

Gaussian beams can be constructed out of BG modes similarly to the way it was done with MBG modes, but with slight modifications. Instead of using the integral (6), we now need [43]

$$\int_0^\infty dx\, x^{n+1} e^{-ax^2} J_n(bx) = \frac{b^n}{(2a)^{n+1}} e^{b^2/4a}, \quad (38)$$

where, contrary to (7), we have to set

$$a = \frac{1}{\kappa} - \frac{1}{\alpha(z)}, \qquad b = \frac{2r}{\alpha(z)}. \quad (39)$$

Let us now define the superposition of BG modes in the form

$$\Psi_s(r,\varphi,z) \overset{\mathrm{def}}{=} \int_0^\infty d\chi \left(\frac{\chi}{\kappa}\right)^{n+1} e^{-\chi^2/\kappa} \Psi_{\mathrm{BG}}^{(n)}(r,\varphi,z). \quad (40)$$

The new condition to be satisfied here is $\mathrm{Re}\kappa < w_0^2$, which ensures the convergence of the integral (40) for an arbitrary value of z. Substituting the explicit formula (37) and exploiting the integral (40), we arrive at

$$\Psi_s(r,\varphi,z) = \frac{1}{[\alpha(z)-\kappa]^{n+1}} r^n e^{in\varphi} e^{-r^2/[\alpha(z)-\kappa]}. \quad (41)$$

Similarly to (8), this expression represents a standard Gaussian beam of nth order with the obvious substitution

$$\alpha(z) \longmapsto \alpha(z) - \kappa, \quad (42)$$

which leads to the modification of the value of the waist $w_0 \mapsto \sqrt{w_0^2 - \mathrm{Re}\kappa}$ and to the shift of the focal plane along the z axis, according to

$$w_0^2 \longmapsto w_0^2 - \mathrm{Re}\kappa, \quad z \longmapsto z - \tfrac{1}{2}k\,\mathrm{Im}\kappa. \quad (43)$$

Apparently it is the same result as in Sec. II A, with merely an inverted sign of the parameter κ. However, it should be kept in mind that modes with completely different properties are now being superposed and also the parameter χ, with respect to which the superposition proceeds, has here a quite different physical sense than earlier. From this perspective, the almost identical result obtained from superpositions (5) and (40) may seem somewhat puzzling. The above effect of the interference of BG beams is attributable to the tightening of the irradiance rings around the propagation axis with increasing value of χ. Simultaneously, a large value of this parameter enforces shifting of the focus to the spot where the imaginary part of the coefficient of χ^2 in the exponent, i.e., $1/\kappa - 1/\alpha(z)$, tends to zero. Otherwise, the destructive interference occurs due to the rapid oscillations of the exponential function.

Let us now pass to the superposition of cofocal BG modes with respect to the topological indices n and choosing a certain constant value of χ. The weighting factors are set, as in Sec. II A, in the form of e^{nv}, dependent on some parameter v,

$$\Psi_s(r,\varphi,z) \overset{\mathrm{def}}{=} \sum_{-\infty}^{\infty} e^{nv} \Psi_{\mathrm{BG}}^{(n)}(r,\varphi,z). \quad (44)$$

The resulting beam can be rewritten in the explicit form as

$$\Psi_s(r,\varphi,z) = \frac{2}{\alpha(z)} e^{(\chi^2-r^2)/\alpha(z)} \sum_{-\infty}^{\infty} e^{n(v+i\varphi)} J_n\left(\frac{2\chi r}{\alpha(z)}\right). \quad (45)$$

Now, using the standard formula for the generating function [44]

$$e^{[z/2](t-1/t)} = \sum_{n=-\infty}^{\infty} J_n(z)t^n, \tag{46}$$

we arrive at

$$\begin{aligned}\Psi_s(r,\varphi,z) &= \frac{2}{\alpha(z)} e^{(\chi^2-r^2)/\alpha(z)} \\ &\quad \times e^{[2\chi r/\alpha(z)](\cos\varphi \sinh v + i\sin\varphi\cosh v)} \\ &= \frac{2}{\alpha(z)} e^{-[1/\alpha(z)][(x-\chi\sinh v)^2+(y-i\chi\cosh v)^2]} \\ &= \Psi^{(0)}_{G\,\mathrm{sh}}(r,\varphi,z).\end{aligned} \tag{47}$$

Thus, the only effect of combining BG modes instead of MBG ones [see Eq. (14)] in the identical manner is to obtain the shifted Gaussian beam by the slightly modified vector

$$\chi[\cosh v, i\sinh v] \longmapsto \chi[\sinh v, i\cosh v]. \tag{48}$$

Now, by picking a purely imaginary value of v, we also get a purely imaginary displacement vector (in the case of superimposing MBG modes it becomes purely real).

The interference mechanism leading to shifted Gaussian beam is similar to that described in Sec. II A with one essential difference. According to (48) for real v the focus is shifted along the x axis either to the right (for v positive) or to the left (for v negative). This was not the case for MBG modes since $\cosh v$ is always positive. This difference is attributable to the following property of the Bessel functions:

$$J_{-n}(z) = (-1)^n J_n(z), \tag{49a}$$

$$I_{-n}(z) = I_n(z). \tag{49b}$$

For BG modes and for positive v the positive-n mode contribution becomes more significant due to the increasing factors e^{nv}. Moreover, destructive interference occurs for the left half plane, i.e., for $x<0$, due to the presence of $e^{in\varphi}$, and constructive interference occurs for the right half plane, i.e., $x>0$. The irradiance peak therefore moves to the right. When $v<0$ the situation is reversed. The negative-n modes contribute more substantially and due to the negative sign in (49a) the destructive interference occurs now for $x>0$. This was not the case when considering the superposition of MBG modes, since the minus sign in (49b) is absent: The destructive interference always takes place for $x<0$, i.e., for any n and any v.

B. Special hyperbolic Bessel-Gaussian beam

Consider now the integral similar to (27) but involving a regular Bessel function [43]

$$\int_0^\infty dx\, e^{-ax^2} J_n(bx) = \sqrt{\frac{\pi}{4a}} I_{n/2}\left(\frac{b^2}{8a}\right) e^{-b^2/8a} \tag{50}$$

and define the superposition

$$\Psi_s(r,\varphi,z) \overset{\mathrm{def}}{=} \int_0^\infty d\chi\, e^{-\chi^2/\kappa}\, \Psi^{(n)}_{\mathrm{BG}}(r,\varphi,z), \tag{51}$$

where $\mathrm{Re}\,\kappa < w_0^2$, as in the preceding section. After having performed the integration we get the expression

$$\begin{aligned}\Psi_s(r,\varphi,z) &= \sqrt{\frac{\pi\kappa}{\alpha(z)[\alpha(z)-\kappa]}} e^{in\varphi} \\ &\quad \times \exp\left(-\frac{r^2}{2\alpha(z)}\frac{2\alpha(z)-\kappa}{\alpha(z)-\kappa}\right) \\ &\quad \times I_{n/2}\left(\frac{\kappa r^2}{2\alpha(z)[\alpha(z)-\kappa]}\right).\end{aligned} \tag{52}$$

If we now redefine the beam's waist and introduce some new parameter χ [as in (30) this designation has nothing to do with the earlier integration variable] according to

$$w_0^2 \longmapsto w_0^2 + \frac{\kappa}{2}, \quad \kappa \longmapsto 2\chi, \tag{53}$$

once again the expression (14) of [49] is obtained.

It may seem somewhat puzzling that the identical superpositions of different beams (MBG and BG beams) yield the same result. It should be noted, however, that the BG and MBG beams are closely related to each other. In fact, they only differ by the replacement of the real integration parameter χ by the purely imaginary one. Since this is the case, it can be concluded that the formulas (28) and (51) describe actually superpositions of the same modes, but one time along the real axis and the other along the imaginary axis of the complex χ. These superpositions can produce the same result as long as the sign of κ is inverted [and it is in fact the only distinction that is revealed in the formulas (29) and (52)] and the integrand function decreases sufficiently fast at infinity (relative to complex χ).

C. Special Laguerre-Gaussian beam

The Laguerre-Gaussian beams are well known in the optical literature, both standard and elegant [3,53]. In this section it will be shown that there exists yet another kind of LG beams, which we provisionally call special LG beams (by their similarity to special hyperbolic BG beams) and which can be obtained by some specific superposition of BG modes. In order to derive the relevant formulas, we use the integral [43]

$$\begin{aligned}&\int_0^\infty dx\, x^{n+2p+1}\, e^{-ax^2} J_n(bx) \\ &\quad = \frac{p!b^n}{2^{n+1}a^{n+p+1}} e^{-b^2/4a} L_p^n\left(\frac{b^2}{4a}\right),\end{aligned} \tag{54}$$

where $L_n^p(z)$ stands for generalized Laguerre polynomial, and consider the superposition

$$\Psi_s(r,\varphi,z) \overset{\mathrm{def}}{=} \int_0^\infty d\chi \left(\frac{\chi}{\kappa}\right)^{n+2p+1} e^{-\chi^2/\kappa} \Psi^{(n)}_{\mathrm{BG}}(r,\varphi,z). \tag{55}$$

Performing the integration according to (54), we get the expression

$$\begin{aligned}\Psi_s(r,\varphi,z) &= \frac{p!\alpha(z)^p}{[\alpha(z)-\kappa]^{n+p+1}} r^n e^{in\varphi} \\ &\quad \times e^{-r^2/[\alpha(z)-\kappa]} L_p^n\left(\frac{\kappa r^2}{\alpha(z)[\alpha(z)-\kappa]}\right).\end{aligned} \tag{56}$$

This kind of a paraxial beam has not been considered so far in the literature and merits some separate detailed examination, which is, however, beyond the scope of the present study.

As in Secs. III A and III B, the convergence of the integral (55) requires that $\mathrm{Re}\kappa < w_0^2$. In the limit of vanishing κ, which is well defined [see the remarks below the formula (5)], the Gaussian beam (4) is restored (apart from a constant factor), due to

$$\lim_{z\to 0} L_p^n(z) = \binom{n+p}{n}. \tag{57}$$

This result is understood if one remembers that any BG beam is composed of inclined Gaussian modes [16]. When $\kappa \to 0^+$, only that with a vanishing value of χ, i.e., that with the wave vector parallel to the z axis, contributes in the superposition (55) owing to the presence of $\exp(-\chi^2/\kappa)$.

D. Generalized paraxial beam

The generalized or few-parameter paraxial beam, which in the hyperbolic version was constructed in Sec. II E out of MBG beams, can also be obtained by a similar superposition of BG beams if the following summation formula [50] is used:

$$\sum_{n=-\infty}^{\infty} e^{in\varphi} J_n(u) J_{m+n}(w) = \left(\frac{w-ue^{-i\varphi}}{w-ue^{i\varphi}}\right)^{m/2} \times J_m(\sqrt{w^2+u^2-2uw\cos\varphi}). \tag{58}$$

The values of the parameters u and w remain at our disposal, so we choose them in a slightly different form than before,

$$u = \mu, \quad w = -\frac{2\chi r}{\alpha(z)}, \tag{59}$$

where μ is a certain real or complex constant. Since $J_n(-z) = (-1)^n J_n(z)$, this implies that

$$\sum_{n=-\infty}^{\infty} (-1)^{n+m} e^{in\varphi} J_n(\mu) J_{m+n}\left(\frac{2\chi r}{\alpha(z)}\right) = e^{-im\varphi}\left(\frac{\xi(x,y,z)}{\eta(x,y,z)}\right)^m J_m(\xi(x,y,z)\eta(x,y,z)), \tag{60}$$

where $\xi(x,y,z)$ and $\eta(x,y,z)$ were defined in (34). Multiplying now both sides of this relation by the factor

$$\frac{1}{\alpha(z)}\, e^{-(r^2-\chi^2)/\alpha(z)+im\varphi} \tag{61}$$

and replacing the summation index n with $n+m$, we arrive at

$$\Psi_s^{(m)}(x,y,z) = \frac{1}{\alpha(z)}\, e^{-(r^2-\chi^2)/\alpha(z)}\left(\frac{\xi(x,y,z)}{\eta(x,y,z)}\right)^m \times J_m(\xi(x,y,z)\eta(x,y,z)) = \sum_{n=-\infty}^{\infty} (-1)^n J_{n-m}(\mu)\Psi_{\mathrm{BG}}^{(n)}(r,\varphi,z). \tag{62}$$

The expression on the left-hand side is a solution of the paraxial equation and constitutes the nonhyperbolic counterpart of the beam derived in [24].

TABLE I. Summary of the expansions.

Beams	MBG	BG
Gaussian	χ integral (5)	χ integral (40)
Gaussian	sum over n (11)	sum over n (44)
γ	χ integral (20)	
KG	χ integral (26)	
special hyperbolic BG	χ integral (28)	χ integral (51)
special LG		χ integral (55)
generalized		sum over n (62)
generalized (hyperbolic)	sum over n (36)	

IV. CONCLUSION

In this work the results on various superpositions of Bessel-Gaussian beams and modified Bessel-Gaussian beams were presented in a fairly systematic way. The dependence of the relevant formulas on two parameters that are under our control, and with respect to which the superpositions can be realized, has been exploited. This seems to be the main benefit of using BG or MBG beams (versus, for example, LG beams): The presence of the extra parameter χ opens up the possibility of constructing with its use superpositions other than those created with respect to the discrete values of orbital angular momentum. An analytical demonstration has been made of how, by selecting appropriate weighting functions for the constituent modes, a number of known beams, both cylindrical and asymmetric in nature, can be generated. It seems that the resulting analytical formulas contribute to a better unified description of different beams and make the connection between various types of solutions to the paraxial equation (1) more apparent, which might also enhance the experimental possibilities of generating certain beams.

By superimposing BG modes, it was possible to construct a beam that has been provisionally termed a special Laguerre-Gaussian beam by analogy with a previously introduced special hyperbolic Bessel-Gaussian beam [49]. A detailed study of this type of mode is left for future work. A summary of the expansions that were possible to obtain in this work is provided in Table I. Additionally, in the Appendix the explicit derivation of the expression (29) describing a certain asymmetric beam is demonstrated by directly solving the paraxial equation.

APPENDIX: EXPLICIT DERIVATION OF THE EXPRESSION (29) FROM THE PARAXIAL EQUATION

In this Appendix the explicit formula (29) will be obtained [in a manner similar to how the formula (52) can be derived] by directly solving the paraxial equation, which in the cylindrical variables has the form

$$\left(\partial_r^2 + \frac{1}{r}\partial_r + \frac{1}{r^2}\partial_\varphi^2 + 2ik\partial_z\right)\Psi(r,\varphi,z) = 0. \tag{A1}$$

Let us first separate the azimuthal dependence by setting

$$\Psi(r,\varphi,z)\frac{1}{\sqrt{\alpha(z)}} e^{in\varphi}\tilde{\Psi}(r,z), \tag{A2}$$

which puts Eq. (A1) in the form

$$\left(\partial_r^2 + \frac{1}{r}\partial_r - \frac{n^2}{r^2} + \frac{2}{\alpha(z)} + 2ik\partial_z\right)\tilde{\Psi}(r,z) = 0. \tag{A3}$$

Now in place of r and z we introduce two new variables

$$\xi = \frac{r^2}{\alpha(z)}, \quad \eta = \frac{1}{\alpha(z)+\kappa}, \tag{A4}$$

where $\alpha(z)$ was defined in (3) and κ is a certain constant. Using these variables Eq. (A3) can be rewritten as

$$\left[\xi\partial_\xi^2 + (1+\xi)\partial_\xi - \frac{(n/2)^2}{\xi} + \frac{1}{2} + \eta^2\left(\frac{1}{\eta} - \kappa\right)\partial_\eta\right]\tilde{\Psi}(\xi,\eta) = 0. \tag{A5}$$

Let us now seek the function $\tilde{\Psi}(\xi,\eta)$ in the form

$$\tilde{\Psi}(\xi,\eta) = \sqrt{\eta}e^{-\xi}\Phi(\tau), \tag{A6}$$

where τ is a new variable defined with $\tau = \frac{1}{2}\kappa\xi\eta$. After having inserted (A6) into (A5), it can be verified that the following *ordinary* differential equation is obtained:

$$\tau\Phi''(\tau) + (1-2\tau)\Phi'(\tau) - \left(\frac{(n/2)^2}{\tau} + 1\right)\Phi(\tau) = 0. \tag{A7}$$

Here primes denote differentiations with respect to the variable τ. The final substitution

$$\Phi(\tau) = e^{\tau}f(\tau) \tag{A8}$$

leads to the modified Bessel equation

$$f''(\tau) + \frac{1}{\tau}f'(\tau) - \left(\frac{(n/2)^2}{\tau^2} + 1\right)f(\tau) = 0, \tag{A9}$$

which has the general solution

$$f(\tau) = C_1 I_{n/2}(\tau) + C_2 K_{n/2}(\tau). \tag{A10}$$

Setting $C_2 = 0$ [the function $K_{n/2}(\tau)$ for $n > 1$ does not lead to a normalizable solution in the perpendicular plane], we can write the complete result in the form

$$\begin{aligned}\Psi(r,\varphi,z) &= \frac{C_1}{\sqrt{\alpha(z)[\alpha(z)+\kappa]}}e^{in\varphi}e^{-r^2/[\alpha(z)+\kappa]} \\ &\quad\times e^{-\kappa r^2/2\alpha(z)[\alpha(z)+\kappa]}I_{n/2}\left(\frac{\kappa r^2}{2\alpha(z)[\alpha(z)+\kappa]}\right) \\ &= C_1\sqrt{\frac{\pi}{\alpha(z)[\alpha(z)+\kappa]}}\,e^{in\varphi} \\ &\quad\times \exp\left(-\frac{r^2}{2\alpha(z)}\frac{2\alpha(z)+\kappa}{\alpha(z)+\kappa}\right) \\ &\quad\times I_{n/2}\left(\frac{\kappa r^2}{2\alpha(z)[\alpha(z)+\kappa]}\right),\end{aligned} \tag{A11}$$

to be compared with (29).

[1] H. Kogelnik and T. Li, Appl. Opt. **5**, 1550 (1966).
[2] L. W. Davis and G. Patsakos, Opt. Lett. **6**, 22 (1981).
[3] See, for instance, A. E. Siegman, *Lasers* (University Science Books, Mill Valley, 1986).
[4] S. Nemoto, Appl. Opt. **29**, 1940 (1990).
[5] L. Mandel and E. Wolf, *Optical Coherence and Quantum Optics* (Cambridge University Press, New York, 1995).
[6] I. Bialynicki-Birula and Z. Bialynicka-Birula, J. Phys. A Math. Theor. **46**, 053001 (2013).
[7] S. R. Seshadri, J. Opt. Soc. Am. A **15**, 2712 (1998).
[8] G. Rodríguez-Morales and S. Chávez-Cerda, Opt. Lett. **29**, 430 (2004).
[9] S. V. Ershkov, J. King Saud. Univ. Sci. **27**, 198 (2015).
[10] M. V. Selina, J. Opt. **49**, 338 (2020).
[11] B. E. A Saleh and M. C Teich, *Fundamentals of Photonics* (Wiley-Interscience, New York, 2007).
[12] C. J. R. Sheppard and T. Wilson, IEE J. Microw. Opt. Acoust. **2**, 105 (1978).
[13] F. Gori, G. Guattari, and C. Padovani, Opt. Commun. **64**, 491 (1987).
[14] A. April, J. Opt. Soc. Am. A **28**, 2100 (2011).
[15] J. Mendoza-Hernández, M. L. Arroyo-Carrasco, M. D. Iturbe-Castillo, and S. Chávez-Cerda, Opt. Lett. **40**, 3739 (2015).
[16] V. Bagini, F. Frezza, M. Santarsiero, G. Schettini, and G. Schirripa Spagnolo, J. Mod. Opt. **43**, 1155 (1996).
[17] L. Allen, M. W. Beijersbergen, R. J. C. Spreeuw, and J. P. Woerdman, Phys. Rev. A **45**, 8185 (1992).
[18] M. Padgett, J. Arlt, N. Simpson, and L. Allen, Am. J. Phys. **64**, 77 (1996).
[19] A. April, Opt. Lett. **33**, 1392 (2008).
[20] A. April, Opt. Lett. **33**, 1563 (2008).
[21] W. Nasalski, J. Opt. **20**, 105601 (2018).
[22] V. V. Kotlyar, R. V. Skidanov, S. N. Khonina, and V. A. Soifer, Opt. Lett. **32**, 742 (2007).
[23] E. Karimi, G. Zito, B. Piccirillo, L. Marrucci, and E. Santamato, Opt. Lett. **32**, 3053 (2007).
[24] T. Radożycki, Phys. Rev. A **106**, 053510 (2022).
[25] D. J. Stevenson, F. J. Gunn-Moore, and K. Dholakia, J. Biomed. Opt. **15**, 041503 (2010).
[26] F. M. Fazal and S. M. Block, Nat. Photon. **5**, 318 (2011).
[27] *Optical Tweezers: Methods and Applications*, edited by M. Padgett, J. Molloy, and D. McGloin (CRC, Boca Raton, 2010).
[28] M. Woerdemann, *Structured Light Fields: Applications in Optical Trapping, Manipulation, and Organisation* (Springer, Berlin, 2012).
[29] R. W. Bowman and M. J. Padgett, Rep. Prog. Phys. **76**, 026401 (2013).
[30] D. G. Grier, Nature (London) **424**, 810 (2003).
[31] V. Kollárová, T. Medřík, R. Čelechovský, Z. Bouchal, O. Wilfert, and Z. Kolka, in *Unmanned/Unattended Sensors and Sensor Networks IV*, edited by E. M. Carapezza, SPIE Proc. Vol. 6736 (SPIE, Bellingham, 2007), p. 368.

[32] C. Altucci, R. Bruzzese, D. D'Antuoni, C. de Lisio, and S. Solimeno, J. Opt. Soc. Am. B **17**, 34 (2000).
[33] M. Nisoli, E. Priori, G. Sansone, S. Stagira, G. Cerullo, S. De Silvestri, C. Altucci, R. Bruzzese, C. de Lisio, P. Villoresi, L. Poletto, M. Pascolini, and G. Tondello, Phys. Rev. Lett. **88**, 033902 (2002).
[34] L. C. Comandar, M. Lucamarini, B. Fröhlich, J. F. Dynes, A. W. Sharpe, S. W.-B. Tam, Z. L. Yuan, R. V. Penty, and A. J. Shields, Nat. Photon. **10**, 312 (2016).
[35] J. Enderlein and F. Pampaloni, J. Opt. Soc. Am. A **21**, 1553 (2004).
[36] C.-F. Li, Opt. Lett. **32**, 3543 (2007).
[37] V. Lakshminarayanan, M. L. Calvo, and T. Alieva, *Mathematical Optics: Classical, Quantum, and Computational Methods* (CRC, London, 2012).
[38] A. Longman and R. Fedosejevs, J. Opt. Soc. Am. A **37**, 841 (2020).
[39] T. Radożycki, Opt. Laser Technol. **147**, 107670 (2022).
[40] B. Patra, *An Introduction to Integral Transforms* (CRC, London, 2018).
[41] A. Erdelyi, *Tables of Integral Transforms* (McGraw-Hill, New York, 1954), Vol. 2.
[42] M. Lax, W. H. Louisell, and W. B. McKnight, Phys. Rev. A **11**, 1365 (1975).
[43] For instance A. P. Prudnikov, Y. A. Brychkov, and O. I. Marichev, *Integrals and Series* (Gordon and Breach, New York, 1986), Vol. 2.
[44] See, for instance, *Handbook of Mathematical Functions with Formulas, Graphs, and Mathematical Tables*, edited by M. Abramowitz and I. A. Stegun (Dover, New York, 1972).
[45] Y. Jiang, S. Zhao, W. Yu, X. Zhu, and X. Zhang, Opt. Commun. **426**, 58 (2018).
[46] C. Koutschan, E. Suazo, and S. K. Suslov, Appl. Phys. B **121**, 315 (2015).
[47] See, for instance, I. S. Gradshteyn and I. M. Ryzhik, *Table of Integrals Series and Products* (Academic, New York, 1980).
[48] T. Radożycki, Phys. Rev. A **104**, 053528 (2021).
[49] T. Radożycki, Phys. Rev. A **104**, 023520 (2021).
[50] G. N. Watson, *A Treatise on the Theory of Bessel Functions* (Cambridge University Press, Cambridge, 1995).
[51] R. Borghi, M. Santarsiero, and M. A. Porras, J. Opt. Soc. Am. A **18**, 1618 (2001).
[52] D. Madhi, M. Ornigotti, and A. Aiello, J. Opt. **17**, 025603 (2015).
[53] T. Takenaka, M. Yokota, and O. Fukumitsu, J. Opt. Soc. Am. A **2**, 826 (1985).